2023 IEEE Symposium Series on Computational Intelligence (SSCI)
Mexico City, Mexico. December 5-8, 2023

Computational Intelligence Driven Motor Function Assessment in Post-Stroke Patients

Illia Yankovyi, Olha Shaposhnyk, Svetlana Yanushkevich
Biometric Technologies Laboratory
University of Calgary, Canada
{illia.yankovyi, olha.shaposhnyk1, syanshk}@ucalgary.ca

MacKenzie Horn, Mohammed Almekhlafi
Cumming School of Medicine and Hotchkiss Brain Institute
University of Calgary, Canada
{mackenzie.horn1, mohammed.almekhlafi1}@ucalgary.ca

***Abstract*—This paper offers an investigation into leveraging computational intelligence (CI) for the assessment of stroke-induced motor weakness in post-stroke survivors, serving as an indicator of neurological function. The proposed methodology deploys deep learning algorithms to analyze video recordings obtained during the post-stroke hospitalization phase. The model effectively categorizes the degree of stroke-induced weakness in the patient's left arm across two and three distinct classes aligned with the National Institutes of Health Stroke Scale. This study was motivated by the limitations of existing monitoring technologies, such as using pressure-sensing mattresses (low resolution and low accuracy). Our long-term strategy is to deploy several means for monitoring the patients' motor function. This study demonstrated a binary classification model using video data collected from a cohort of 23 post-stroke patients in a clinical setting for 48 hours. Employing a 3-fold cross-validation methodology, the developed model showcases an accuracy rate of $92.10 \pm 4.08\%$ for the binary classification, distinguishing between mild and severe stroke-induced weakness in the left arm. In the case of three classes, the model achieves an accuracy of $89 \pm 4.95\%$.**

***Index Terms*—deep learning, stroke diagnosis, motion impairment, human motion analysis.**

I. Introduction and objectives

A stroke is a life-threatening cerebrovascular disease that can cause long-term disabilities. Timely identification and early intervention are crucial in preventing permanent brain damage, motor function impairment, or fatal outcomes. The initial hour following stroke onset is particularly critical, as it presents the optimal window for administering medication and increasing the likelihood of favorable patient outcomes. Moreover, hospitalized stroke patients are at risk of recurrence, with approximately 50% of recurrent strokes occurring within the first two weeks of the initial stroke [1]. Throughout stroke treatment, a patient's motor function can recover or deteriorate.

The results from study [2] demonstrate a potential 14% rate of missed diagnosis of ischemic stroke in the USA, while another study [3] reports a 12% rate of delayed stroke diagnosis in Japan. These findings emphasize the importance of enhancing diagnostic accuracy and timeliness in stroke across diverse healthcare settings. Delayed diagnoses can lead to prolonged hospitalization duration and undesirable outcomes for stroke patients.

A fundamental manifestation of stroke is motor weakness, often accompanied by compromised limb mobility. A substantial majority, approximately 77%, of individuals afflicted by stroke encounter some degree of upper extremity weakness [4]. The conventional approach to assessing stroke-associated weakness involves motor assessments. Unfortunately, this bedside evaluation method remains partly subjective, can disrupt patients, and may lack consistent sensitivity to capture noteworthy alterations. The frequent and routine hourly monitoring of patients at the bedside burdens both patients and healthcare providers, contributing to inefficiencies in medical resource use and increasing fatigue in patients.

Consequently, there is a need for a non-intrusive computational intelligence (CI) tool that can consistently gauge the extent of stroke-induced motor weakness at the patient's bedside. Such a system would effectively overcome the constraints associated with subjective bedside evaluations. It would also streamline the laborious process of frequent monitoring, thereby improving patient care.

The rest of the paper is organized as follows. We formulate the problem in Section II, and discuss the related research in the field in Section III. The proposed approach is explained in Section IV, and the results are reported in Section V, followed by discussion, conclusions, and suggestions for future work (Section VI).

II. Problem formulation and idea of approach

Medical practitioners anticipate the technology that can non-invasively track body motion to monitor the neurological status of hospitalized stroke survivors. This status changes dramatically in the first 72 hours after admission and usually manifests via reduced body movements affecting one side of the body. The requested technology must complement the capabilities of medical practitioners in accurately, consistently, and continuously detecting neurological deterioration or improvement and any changes in motor function during the post-stroke period or longer periods, and at times when the continuous practitioners' supervision is not present or possible. This will lead to faster diagnosis, personalized treatments, better outcomes, and net savings in the healthcare system.

Various technologies were proposed to satisfy the condition of non-invasiveness. The pressure signature provided by sensory mats was investigated for the ability to capture the impact of neurological deterioration in 2D space to a certain extent affected by body weights, position, etc. Previous experimental sondage [5] showed that additional sources of information are needed to extract these features. The negative effects of the pressure data ambiguity resulted in both the low resolution and low accuracy. Our strategy to mitigate and compensate for these limitations of pressure-sensing mattresses is to use data from multi-spectral monitoring devices. This strategy is schematically represented as follows:

$$\underbrace{\left\{\begin{array}{c}\texttt{Pressure}\\ \texttt{Signature}\end{array}\right\}}_{\textit{Sensing mattress}} \Rightarrow \texttt{Fusion} \Leftarrow \underbrace{\left\{\begin{array}{c}\textbf{Skeleton}\\ \textbf{Signature}\end{array}\right\}}_{\substack{\textbf{\textit{Camera monitoring}}\\ \textbf{\textit{(This paper)}}}} \tag{1}$$

where the right side of the diagram represents the contribution of this paper. The long-term goal is to conduct a fusion of the two approaches in order to create a more complete map of the neurological deterioration of a stroke survivor in the first 72 hours in hospital settings. This map is a guide for further development of the personalized rehabilitation process, for example, exoskeleton-based rehabilitation [6], [7], [8]. Surveillance of a stroke survivor in the infrared spectrum (at night) is not considered in this work. The privacy of video records is addressed by extracting and displaying the body joints, or key points, in lieu of the video images.

III. Related Works

In the prior research into CI-based action recognition pertinent to stroke and various neurological disorders, several approaches were developed [9], such as analyzing data captured by wearable devices, analyzing the pressure sensors data, and video monitoring. The wearable technology-driven approach has emerged as a widespread method in action recognition research [10]. It also showed effectiveness in identifying the early symptoms of stroke [11], [12], [13]. This approach gained popularity through the usage of smartwatches, fitness trackers, and other devices worn on the body or integrated into clothing. These devices are equipped to monitor diverse physiological signals, which enable tracking of health metrics, movement, and conditions. However, these devices are useful as additional data sources for pressure-sensing mattresses.

Pressure sensor arrays positioned a top mattress function by quantifying alterations in pressure distribution when an individual assumes a lying or sitting position. Recent studies attempted to employ the recorded data medical analysis, such as post-stroke motor function assessment [5], [14] or sleep apnea events detection [15]. This technology exhibits significant drawbacks, such as low resolution and high cost. Other drawbacks include the incapacity to collect data when the patient is not reclining on the sensor surface or when extraneous objects, such as a pillow, a book, or a laptop, are present on the mattress. Hence, an additional source of data is needed, such as video monitoring. The multi-source approach is beneficial because it mitigates strong requirements for a pressure-sensing mattress and does not require high accuracy of pose recognition from video surveillance data. However, these benefits must be confirmed in the third phase of the project, i.e., the fusion of images of a lying patient from cameras and mattresses.

Significant advancements have been achieved in the last few decades in the area of biomechanical analysis of human motion in the context of neurological injuries such as stroke, cerebral palsy, Parkinson's disease [16], [17], [18], [19]. A system for detection of stroke effects has been described in [20], which aims to assess facial symmetry, arm weakness, and speech difficulty in real-time using 3D joint coordinates recorded with depth cameras known as a Kinect-like platform. It is possible to use this platform for the purpose of our project, but it is a costly solution.

IV. System for Continuous Monitoring of Neurological Status of Stroke Survivors

The system for continuous monitoring of the neurological status of stroke survivors includes pre-processing and keypoint feature extraction (Figure 1). The features are then fed into a deep neural network chosen as a model for the classification of the motor function. We restricted the analyzed data to the upper body (arms) since bed-ridden patients usually have their lower bodies covered by a blanket. Finally, the degree of motor weakness using the data from the video is identified.

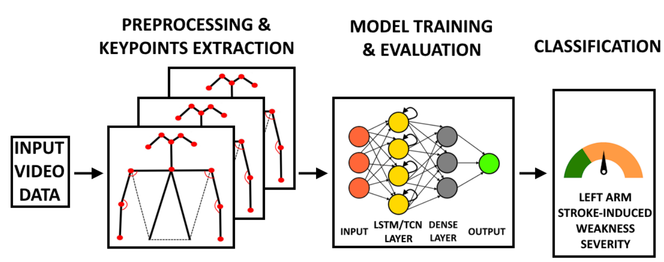

Fig. 1: An approach to data processing and motor function classification using data from video monitoring of stroke survivors.

A. Dataset and pre-processing

The dataset was gathered through a collaborative effort of the Biometric Technologies Laboratory and the Stroke Unit at the Foothills Medical Centre in Calgary. The research group obtained ethics approval for data collection in this study from the Conjoint Health Research Ethics Board. The study cohort comprised 23 post-stroke individuals. The patients were not provided with specific instructions. For each patient, the monitoring process was performed over a period of up to three days, resulting in a collection of video records. Within these videos, the subjects were observed lying on the bed in a clinical setting, with a blanket covering the lower part of their bodies. Among the patients, 14 exhibited left-sided weakness, six had right-sided weakness, and three did not present any signs of stroke-induced weakness upon initial assessment. The dataset for the study reported in this paper was collected using the Wyze Cam v2 video camera. The camera provides 15 frames per second with 1080p resolution

(1920×1080) at a 110-degree viewing angle. The raw video data was divided into short fragments of 60 seconds each.

The dataset utilizes the National Institutes of Health Stroke Scale (NIHSS) as the ground truth (the annotation metric) for evaluating the severity of motor weakness, with a single value recorded per day. The NIHSS is utilized by healthcare providers to objectively quantify the degree of stroke-induced impairment based on a manual patient assessment. NIHSS comprises 11 items that score abilities on a scale of 0 to 4. The list of instructions for the NIHSS includes but is not limited to an assessment of the ability to hold the left/right and upper/lower extremities without any movement drift after 5 seconds for legs and after 10 seconds for arms. It also includes a limb ataxia test using the finger-nose-finger and heel-shin tests. In addition, NIHSS includes specific non-motoric-related tests that reflect the patient's neurological function. Higher NIHSS scores indicate more severe impairment, while 0 signifies normal function. The total NIHSS score is obtained by adding the item scores; the total score values range from 0 to 42.

The stroke severity index is classified into five distinct classes, determined by the NIHSS score. Among the complete cohort of 23 stroke patients, the distribution of these classes unfolded as follows: 14 patients classified as 'mild stroke', 9 patients classified as 'moderate stroke', and no patients in the remaining categories. Table I provides details of the initial data used in the experiment

TABLE I: The number of patients and the number of frames collected for each of the stroke severity classes.

Severity	Total NIHSS	# Frames	# Patients
Mild stroke	1-4	665 000	14
Moderate stroke	5-15	576 000	9

A data-cleaning procedure is essential before applying any classification model. The dataset preprocessing involved the exclusion of specific fragments to enhance the data quality for subsequent analyses and model development. These fragments consisted of instances where patients were not visible in the video frames and periods characterized by minimal or no movement, typically during sleep, as these segments were deemed irrelevant for subsequent data processing. By removing these segments, the dataset was refined to focus on informative data, thus ensuring the reliability of subsequent analyses and model development. Given the presence of temporal gaps within the recording, the dataset lacks complete continuity and is partitioned into sequential segments (sessions). When assessing motor weakness severity using fixed-sized, non-overlapping, and consecutive time intervals (tumbling windows), we obtained a number of time windows, which could be insufficient for deep learning techniques usage. To overcome this limitation and to enrich the data, we utilized a sliding window approach with a window length of 500 rows and a step of 100 rows. By doing this, we generated a temporal windows quantity that was increased by an order of magnitude.

As indicated in Table II, it becomes evident that the instances of left arm NIHSS values are not uniformly distributed. As a result, we have established discrete groupings according to the ranges of NIHSS values specific to the left arm.

In our study, two types of models were investigated: a 2-class classification (categorized by motor component of the NIHSS values: 0-2 with 33.34% of all data, 3-4 with 66.66% respectively) and a multi-class classification (categorized by NIHSS values: 0-1 with 20.55%, 2-3 with 34.34%, 4 with 45.11%).

B. Deep learning of motor functions

At the data preparation stage, face blurring of the individuals involved in the study was applied to maintain compliance with ethical guidelines and data protection regulations. The prepared dataset consists of body keypoint coordinates (skeleton joints) and elbow and shoulder joint relative angles and does not contain any sensitive information. This study utilized a Python-based deep-learning pipeline to address the classification task. The data pipeline consists of several key steps, including pre-processing raw video surveillance data, extracting human pose features, and training time series algorithms.

Videos were downsampled to one frame per second to maintain a manageable dataset size. Frames were extracted and saved as separate images from each one-minute video segment. A region of interest with the patient's location was identified with the object detection model faster RCNN R-50-FPN [21]. Due to the presence of blankets covering the lower extremities of most patients, the study focused on the estimation of upper body skeletal joints' coordinates. This was accomplished using the state-of-the-art pre-trained human pose estimation model, the High-resolution network (HRNet) [22].

Subsequent to this initial phase, a data smoothing process was undertaken to address inherent limitations in the skeleton point recognition algorithm, which fails to achieve absolute precision. The Savitzky–Golay filter [23], recognized for its capacity to enhance data precision without compromising underlying signal trends, was employed to achieve this. After a series of experimental iterations employing diverse window sizes, a window size of 13 was determined as optimal. Then, shoulder and elbow angles were calculated for both sides of each subject body. The resulting dataset comprises 24 columns, including 20 values representing coordinates for 10 pose keypoints and four relative joint angles (left and right elbow, left and right shoulder).

The Multivariate Imputation by Chained Equations (MICE) [24] algorithm was applied to handle missing data points. This was followed by data normalization. Features were normalized to rescale the values in each column within the range [0,1].

In this study, we investigated two deep learning time-series processing architectures: Long Short-Term Memory (LSTM [25]) and Temporal Convolutional Network (TCN [26]) trained on skeletal key points and joint angles to classify the severity of stroke-induced weakness

TABLE II: The data distribution shows the prevalence of left arm motor weakness in stroke survivors dataset, categorized by severity levels.

NIHSS value	Duration (seconds)	Fraction of all data, %	Description
0	67500	19.40	No drift, limb bends for 5 seconds
1	4000	1.15	Drift down before full 5 seconds; does not hit the bed
2	44500	12.79	Drift; limb hits the bed, some effort against gravity
3	75000	21.55	No effort against gravity, limb falls
4	157000	45.11	No movement

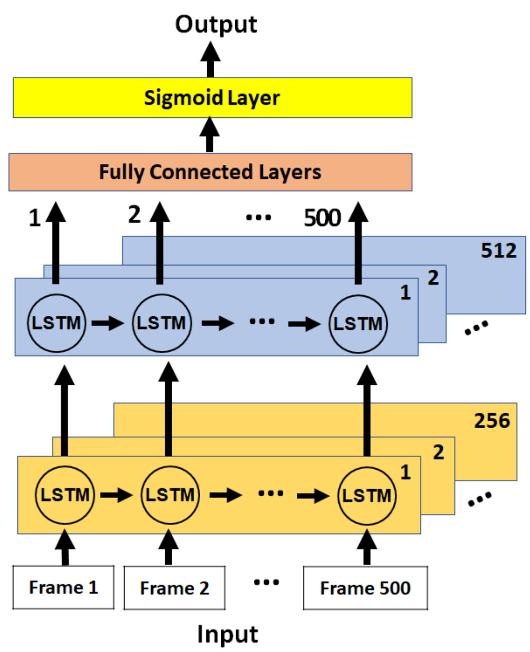

Fig. 2: The proposed deep learning model architecture classifies the severity of stroke-induced motor weakness into two classes: "mild stroke" or "moderate stroke".

These models were trained using 500-second long windows and mini-batch gradient descent with a batch size of 64 samples using AMSGrad optimizer with an initial learning rate of 0.002. The latter was the variability parameter, which decreased using learning rate decay to 0.000001. A loss function for two classes is a binary cross-entropy, and for three classes, it is a categorical cross-entropy.

The investigated architecture options consist of two and one LSTM layer or one TCN module applied to process time-series data, followed by one or three dense layers with a dropout rate of 0.3. The output layer employs a sigmoid activation function and has a single node for binary classification or three nodes (applying one-hot encoding) for multi-classification (three classes). Using the proposed model, a 3-fold cross-validation was performed using Group k-fold to avoid leaking the same data to both train and test datasets. The dataset was split into a training set (33.3%) and a test set (66.7%). The network was trained on GPU NVIDIA Tesla T4 on the Google Colaboratory platform.

The pre-trained on COCO dataset, Faster R-CNN model with a ResNet-50-FPN backbone is applied to detect a region in the frame containing the image of the subject. Then, pre-trained High-resolution network HRNet [27] W48 is used to detect body joints and extract features related to posing. The coordinates of the joints are used for relative joint angle calculation and further movement analysis. We repeat this procedure for one frame per second and quantify the amount of movement made by each upper extremity of the subject. The sequence of calculated values is used to estimate the overall motor skill dynamic and to calculate a ratio of movement between the right/left sides of the body. During the next step, the LSTM and TCN were trained to classify the severity of subjects' motor weakness.

Figure 2 illustrates the proposed approach to stroke-induced weakness severity monitoring by analysis of the subject pose using LSTM.

The system's primary objective is to accurately classify the patient video data into distinct categories representing different levels of motor weakness severity that are based on the corresponding NIHSS scores. A human movement tracking system detects a box containing a person and analyzes changes in its pose, movements of joints, and relative joint angles over time.

For the assessment of model accuracy, we employed the subsequent metrics: True Positives (TP) – the number of correctly labeled subjects with no to mild motor weakness symptoms; False Negatives (FN) – the number of subjects with severe motor weakness symptoms incorrectly labeled as no to mild motor symptoms; True Negatives (TN) – the number of correctly labeled subjects with severe motor weakness symptoms; and False Positives (FP) – the number of subjects with no to mild motor weakness symptoms incorrectly labeled as severe motor weakness. Using these measures, the ensuing performance indicators were calculated using the following equations: $\texttt{Accuracy}$=(TP+TN)÷(TP+FN+TN+FP); $\texttt{Recall}$=TP÷(TP+FN); $\texttt{Precision}$=TP÷(FP+TP).

V. Experimental Assessments of Motor Functions

This section describes the performance evaluation of the deep learning architecture under diverse hyperparameter configurations. The dropout rate (0.3 or 30%), the initial learning rate (0.002), the final learning rate (0.000001), and L2 regularization (0.001) after each Dense layer were determined experimentally. A comparative analysis was conducted to assess the performance of models utilizing LSTM and TCN for different depths of layers processing the temporal information and a different number of the following dense layers.

Through experimentation, some models exhibited erratic behavior, displaying instances of highly variable results when subjected to training on different fractions of the dataset. To address this issue, 3-Fold Group cross-validation was explored as a potential solution. Group k-fold cross-validation is used when specific groups or clusters within the data must be kept together to avoid information leakage. We ensure the model will learn inter-patient patterns by choosing patient ID as the group. However, as illustrated in Table III for the 2-class and Table IV for the 3-class classification, specific models exhibit these deviations across folds, implying potential imbalances in data distribution or deficiencies in representation within the subject population for each class.

TABLE III: Binary classification (NIHSS 0-2 against NIHSS 3-4 for a left arm motor drift): the effect of time series processing architecture and a number of dense layers on classification accuracy, macro precision, and macro recall. The values in bold represent the best performance.

Temporal Layers	№ Dense Layers	Accuracy	Precision (macro)	Recall (macro)
1 LSTM	3	69.40 ±15.30	50.25 ±13.63	54.34 ±6.13
2 LSTM	1	56.32 ±13.57	54.49 ±24.56	57.01 ±5.18
2 LSTM	3	70.83 ±26.02	79.60 ±15.60	67.58 ±25.75
1 TCN	1	**92.10 ±4.08**	**89.08 ±5.62**	**92.12 ±4.37**
1 TCN	3	83.05 ±14.49	83.91 ±13.63	87.71 ±7.27

TABLE IV: 3-class classification (NIHSS 0-1 against NIHSS 2-3 against NIHSS 4 for a left arm motor drift): the effect of the architecture of time series processing layers and the number of dense layers on classification accuracy, macro precision, and macro recall.

Temporal Layers	# Dense Layers	Accuracy	Precision (macro)	Recall (macro)
1 LSTM	3	37.36 ±14.79	32.60 ±16.23	27.67 ±7.90
2 LSTM	1	41.38 ±22.57	41.09 ±8.09	37.56 ±15.14
2 LSTM	3	58.62 ±14.66	37.79 ±16.79	47.65 ±14.64
1 TCN	1	74.71 ±22.29	81.87 ±13.10	73.39 ±20.55
1 TCN	3	**89.00 ±4.95**	**90.21 ±5.27**	**85.35 ±6.87**

In both 2-class and 3-class tasks, LSTM-based models generally underperformed compared to TCN-based models. Despite its faster training speed, the LSTM model was prone to overfitting. The optimal binary classification performance was achieved by a model featuring a single TCN layer followed by a single Dense layer, as shown in Figure 3 depicting its corresponding confusion matrix. Similarly, the best performance in the 3-class classification scenario was exhibited by a model comprised of a single TCN layer followed by three Dense layers, as reflected in Figure 4 depicting its associated confusion matrix.

VI. Discussion, Conclusion and Future Work

This work contributes to the study of non-invasive approaches according to the strategy (1) proposed by the co-authors to assist the medical practitioners in assessing the changes in stroke-induced motor weakness of stroke survivors in a hospital environment. The urgency in developing and improving such technology is motivated by the number

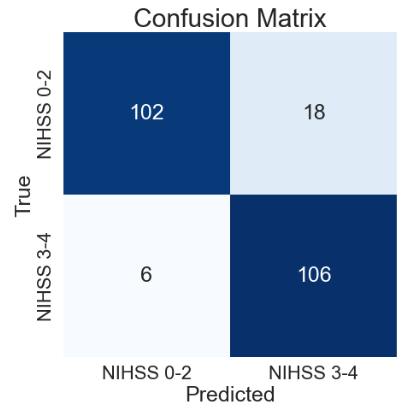

Fig. 3: The confusion matrix for the two-class model with 500-long input sequence, one TCN layer, one dense layer, dropout rate of 0.3, sigmoid output function, and binary cross-entropy loss function.

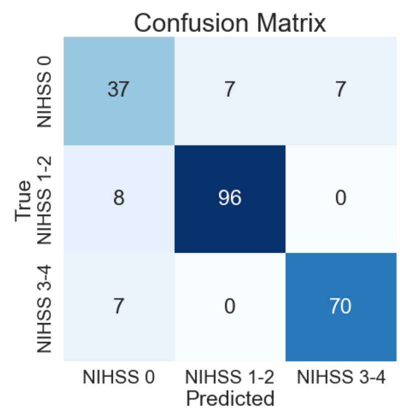

Fig. 4: The confusion matrix for the three-class model with 500-long input sequence.

of strokes registered every year (for example, there were 13.7 million strokes in 2019 [28] in the USA).

Our ongoing investigation aims to prove the feasibility of a classification tool based on deep learning for evaluating the severity of neurological functions in post-stroke patients over time using video data. The system uses human pose estimation algorithms to retrieve skeleton joint coordinates and calculate joint relative angles. This data is used by time series deep learning models to classify the severity of stroke-induced weakness. We tested two models: LSTM and TCN, with different numbers of layers and found that TCN performed better. The conclusion is that in both 2-class and 3-class tasks, LSTM-based models generally underperformed compared to TCN-based models.

Limitations: There are several limitations to the reported results. The sample of stroke patients was small, and some video frames were unusable due to obstruction, location, and low-light conditions. These factors, as well as biases of pre-processing, impacted the performance of the deep learning model.

Conclusion: The key conclusion from our study is that the CI-based processing of video data is a feasible yet insufficient source for performing an accurate assessment of the stroke patient's motor function in a clinical setup. Other challenges arise from potential occlusions and reliance on camera positioning, which may impede effective data processing.

Future work: Next steps according to our strategy (1) include a) an extension of the approach by using infrared videos (night-time monitoring), and b) a fusion of video data with pressure sensory data. Another suggestion for improving the model by providing the data sufficient for training the models [29] is generating the synthetic video frames, body joint points, and pressure maps.

ACKNOWLEDGMENT

This research was supported in part by the Natural Sciences and Engineering Research Council of Canada (NSERC), Mitacs (Canada), and the University of Calgary Vice-President (Research) Catalyst Grant.

REFERENCES

[1] H. Erdur, J. F. Scheitz, M. Ebinger et al., In-hospital stroke recurrence and stroke after transient ischemic attack: Frequency and risk factors, *AHA Stroke*, vol. 46, no. 4, pp. 1031–1037, 2015.

[2] A. E. Arch, D. C. Weisman, S. Coca et al., Missed Ischemic Stroke Diagnosis in the Emergency Department by Emergency Medicine and Neurology Services, *Stroke*, vol. 47, no. 3, pp. 668–673, 2016.

[3] C. Takarada, J. Komagamine, and T. Mito, Prevalence of delayed diagnosis of acute ischemic stroke in an acute care hospital: A single-center cross-sectional study in Japan, *Journal of General and Family Medicine*, vol. 22, no. 5, pp. 262–270, 2021.

[4] J. van Kordelaar, E. E. van Wegen, R. H. Nijland et al., Assessing Longitudinal Change in Coordination of the Paretic Upper Limb Using On-Site 3-Dimensional Kinematic Measurements, *Physical Therapy and Rehabilitation Journal*, vol. 92, no. 1, pp. 142–151, 2012.

[5] H. C. R. Oliveira, H. Altaf, M. Almekhlafi et al., Pressure Sensor Data Analysis for Motor Function Assessment of Stroke Patients, *IEEE Symposium Series on Computational Intelligence (SSCI)*, pp. 551–558, 2022.

[6] A. Anastasiev, H. Kadone, A. Marushima, H. Watanabe, A. Zaboronok, *et. al.* Supervised Myoelectrical Hand Gesture Recognition in Post-Acute Stroke Patients with Upper Limb Paresis on Affected and Non-Affected Sides, *Sensors*, vol.22 issue 8733, 2022.

[7] C. J. W. Haarman, E. E. G. Hekman, J. S. Rietman, and H. Van Der Kooij, Mechanical design and feasibility of a finger exoskeleton to support finger extension of severely affected stroke patients, *IEEE Trans. Neural Syst. Rehabilitation Eng.*, vol.31, pp. 1268–1276, 2023.

[8] J. de Miguel-Fernandez, C. Pescatore, A. Mesa-Garrido, C. Rikhof, E. Prinsen, *et al.,* Immediate Biomechanical Effects of Providing Adaptive Assistance with an Ankle Exoskeleton in Individuals After Stroke, *IEEE Robotics and Automation Letters*, vol.7, no. 3, pp. 7574–7580, 2022.

[9] S. Sardari, S. Sharifzadeh, A. Daneshkhah et al., Artificial Intelligence for skeleton-based physical rehabilitation action evaluation: A systematic review, *Computers in Biology and Medicine*, vol. 158, p. 106835, 2023.

[10] Y. Wang, S. Cang, and H. Yu, A survey on wearable sensor modality centred human activity recognition in health care, *Expert Systems with Applications*, vol. 137, pp. 167–190, 2019

[11] J. Wasselius, E. Lyckegard Finn, E. Persson et al., Detection of Unilateral Arm Paresis after Stroke by Wearable Accelerometers and Machine Learning, *MDPI Sensors*, vol. 21, no. 23, p. 7784, 2021.

[12] M. Wallich, K. Lai, and S. Yanushkevich, Assessing Upper Limb Motor Function in the Immediate Post-Stroke Period Using Accelerometry, *IEEE Conference on Artificial Intelligence (CAI)*, pp. 132–133, 2023.

[13] N. Razfar, R. Kashed, and F. Mohammadi, Post-Stroke Virtual Assessment Using Deep Learning, *IEEE Conference on Artificial Intelligence (CAI)*, pp. 116–117, 2023.

[14] N. Abid, P. Kozlow, and S. Yanushkevich, Detection of Asymmetric Abnormalities in Gait using Depth Data and Dynamic Bayesian Networks, *14th IEEE International Conference on Signal Processing (ICSP)*, pp. 762–767, 2018.

[15] H. Azimi, P. Xi, M. Bouchard et al., Machine Learning-Based Automatic Detection of Central Sleep Apnea Events From a Pressure Sensitive Mat, *IEEE Access*, vol. 8, pp. 173428–173439, 2020.

[16] S. L. Colyer, M. Evans, D. P. Cosker et al., A Review of the Evolution of Vision-Based Motion Analysis and the Integration of Advanced Computer Vision Methods Towards Developing a Markerless System, *Sports Med.*, vol. 4, no. 1, p. 24, 2018.

[17] B. Scott, M. Seyres, F. Philp et al., Healthcare applications of single camera markerless motion capture: a scoping review, *PeerJ*, vol. 10, p. e13517, 2022.

[18] E. Martini, N. Valè, M. Boldo et al., On the Pose Estimation Software for Measuring Movement Features in the Finger-to-Nose Test, *IEEE International Conference on Digital Health (ICDH)*, pp. 77–86, 2022.

[19] B. X. B. Yu, Y. Liu, K. C. C. Chan et al., Skeleton-based human action evaluation using graph convolutional network for monitoring Alzheimer's progression, *Pattern Recognition*, vol. 119, p. 108095, 2021

[20] V. Ramesh, S. Kim, H.-A. Nguyen, K. Agrawal, B. C. Meyer, and N. Weibel, "Developing Aids to Assist Acute Stroke Diagnosis," *Extended Abstracts of the 2020 CHI Conference on Human Factors in Computing Systems*, pp. 1–7, April 2020.

[21] S. Ren, K. He, R. Girshick et al., Faster R-CNN: Towards Real-Time Object Detection with Region Proposal Networks, *Advances in Neural Information Processing Systems*, vol. 28, 2015.

[22] K. Sun, B. Xiao, D. Liu, et al., Deep High-Resolution Representation Learning for Human Pose Estimation, *IEEE/CVF Conference on Computer Vision and Pattern Recognition (CVPR)*, pp. 5686–5696, 2019.

[23] R.W. Schafer, What Is a Savitzky-Golay Filter? *IEEE Signal Processing Magazine*, vol. 28, no. 4, pp. 111–117, 2011.

[24] M. J. Azur, E. A. Stuart, C. Frangakiset et al., Multiple imputation by chained equations: what is it and how does it work?, *International Journal of Methods in Psychiatric Research*, vol. 20, no. 1, pp. 40–49, 2011.

[25] S. Hochreiter and J. Schmidhuber, Long Short-Term Memory, *Neural Computation*, vol. 9, no. 8, pp. 1735—1780, 1997.

[26] C. Lea, M. D. Flynn, R. Vidal et al., Temporal Convolutional Networks for Action Segmentation and Detection, *Proceedings of the IEEE Conference on Computer Vision and Pattern Recognition*, pp. 156–165, 2017.

[27] J. Wang, K. Sun, T. Cheng et al., Deep High-Resolution Representation Learning for Visual Recognition, *IEEE Transactions on Pattern Analysis and Machine Intelligence*, vol. 43, no. 10, pp. 3349–3364, 2021.

[28] M. P. Lindsay, B. Norrving, R. L. Sacco et al., World Stroke Organization (WSO): Global Stroke Fact Sheet 2019, *Int J Stroke*, vol. 14, no. 8, pp. 806–817, 2019.

[29] I. Boukhennoufa, D. Jarchi, X. Zhai, V. Utti, S. Sanei, T. K. M. Lee, Jo. Jackson, and K. D. McDonald-Maier, A novel model to generate heterogeneous and realistic time-series data for post-stroke rehabilitation assessment, *IEEE Trans. Neural Systems and Rehabilitation Engineering*, 2023, Vol.31, p.2676–2687.